JACS
JOURNAL OF THE AMERICAN CHEMICAL SOCIETY

Communication

pubs.acs.org/JACS

One-Step Construction of Two Different Kinds of Pores in a 2D Covalent Organic Framework

Tian-You Zhou, Shun-Qi Xu, Qiang Wen, Zhong-Fu Pang, and Xin Zhao*

Key Laboratory of Synthetic and Self-Assembly Chemistry for Organic Functional Molecules, Shanghai Institute of Organic Chemistry, Chinese Academy of Sciences, 345 Lingling Road, Shanghai 200032, China

Supporting Information

ABSTRACT: Covalent organic frameworks (COFs) are crystalline porous materials bearing microporous or mesoporous pores. The type and size of pores play crucial roles in regulating the properties of COFs. In this work, a novel COF, which bears two different kinds of ordered pores with controllable sizes: one within microporous range (7.1 Å) and the other in mesoporous range (26.9 Å), has been constructed via one-step synthesis. The structure of the dual-pore COF was confirmed by PXRD investigation, nitrogen adsorption−desorption study, and theoretical calculations.

Covalent organic frameworks (COFs),[1−4] which are porous and crystalline polymers with predictable structures, have drawn a great deal of interest recently because of their important applications in gas storage and separation,[5,6] catalysis,[7,8] and electronic devices.[9−11] Since the pioneering work of Yaghi in 2005,[1] a variety of COFs have been constructed by utilizing different linkages such as boronate,[12−14] imine,[7,15−18] and hydrazone.[19] A notable feature of these linkages is that they are formed by dynamic covalent bonds,[20] which are reversible under certain conditions and thus allow self-repairing to occur to generate polymeric network with highly ordered internal structures. In this context, the preparation of COFs usually gives thermodynamically the most stable structures.

One distinctive feature of two-dimensional (2D) COFs is their inherent porosity, which comes from well-defined pores periodically spreading in 2D sheets. It is the pores that endow COFs with the versatile applications. Although the size and shape of pores in a 2D COF can be well tailored by changing the structures of monomers,[21−24] the introduction of different kinds of pores into a COF is still a great challenge. One reason is that it is extremely hard to simultaneously control the formation of two pores bearing different sizes. Furthermore, polymorphism might arise, which usually results in several topological structures at the same time. To address this challenge, delicate design of monomers is required. In this communication, we report one-step construction of a dual-pore COF bearing two different kinds of pores,[25] in which hexagonal pores (26.9 Å) and triangle pores (7.1 Å) are alternately and periodically arranged (Scheme 1). To the best of our knowledge, this is the first 2D COF having both micropores and mesopores with predictable sizes.

Scheme 1. Synthesis and Structure of the Dual-Pore COF

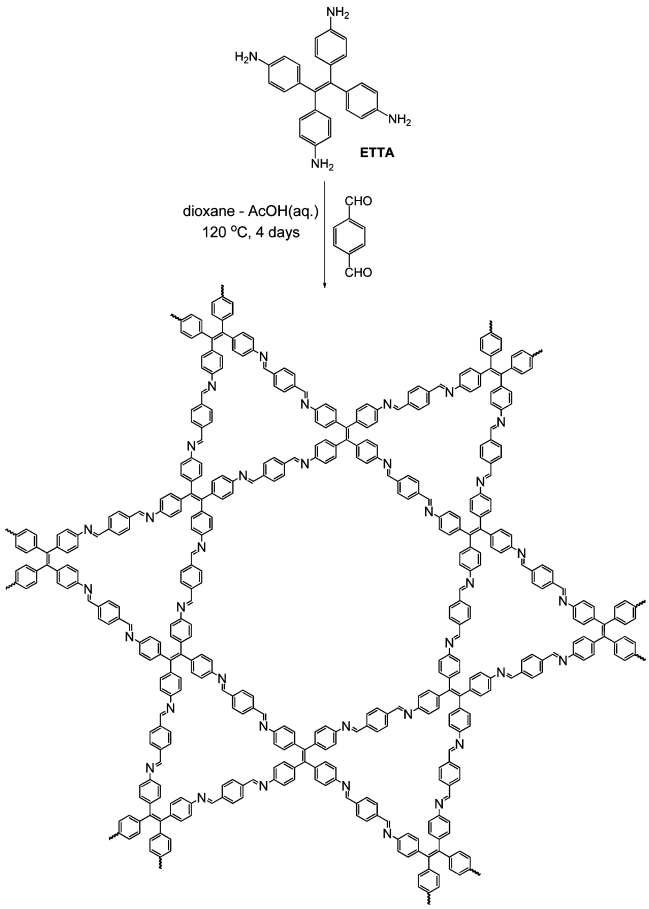

From the topological point of view, it is anticipated that combination of a D_{2h} symmetric monomer and a C_2 symmetric monomer would result in two crystallographic systems: one is an orthorhombic system that bears only a single uniform size of pores in its periodic framework, and the other is a hexagonal system that possesses two different kinds of pores. Furthermore, each of the systems can be further divided into two structures: eclipsed and staggered. Therefore, there will be four possible structures that can be generated. Under thermodynamic control conditions, the product distribution is

Received: September 9, 2014
Published: October 31, 2014

dx.doi.org/10.1021/ja5092936 | J. Am. Chem. Soc. 2014, 136, 15885−15888

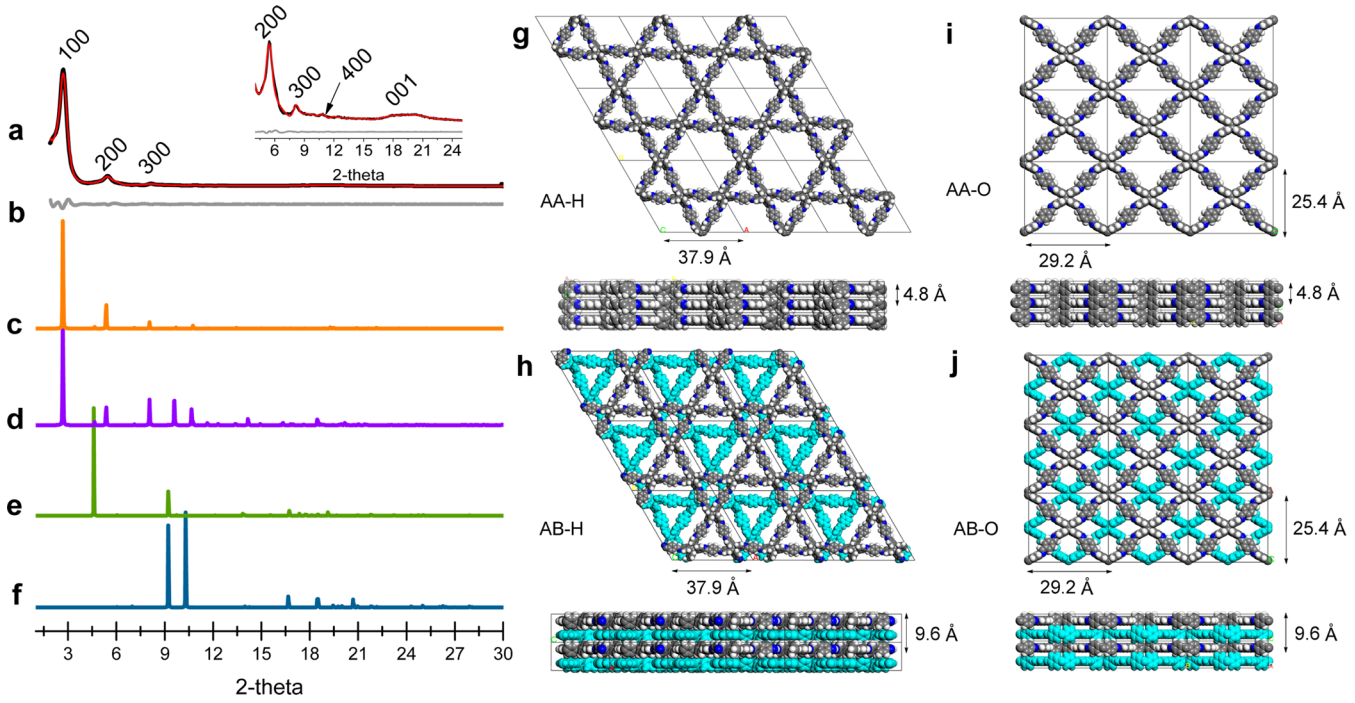

Figure 1. Left: (a) Experimental (black) and refined (red) PXRD pattern of the as-prepared COF. (b) Difference plot between the experimental and refined PXRD patterns (gray). (c) Simulated PXRD pattern for **AA-H** structure, (d) **AB-H** structure, (e) **AA-O** structure, and (f) **AB-O** structure. Right: (g) **AA-H** structure, (h) **AB-H** structure, (i) **AA-O** structure, and (j) **AB-O** structure, all with the unit cell parameters.

determined by the energy difference of the products. Therefore, the one with the lowest energy could be the only product produced if the energy difference between it and the other products is large enough. To this end, as a proof-of-concept project, we selected 4,4′,4″,4‴-(ethene-1,1,2,2-tetrayl)-tetraaniline (**ETTA**) as the D_{2h} symmetric monomer and terephthalaldehyde as the C_2 symmetric monomer. The condensation reaction between them was carried out under solvothermal conditions. Thus, heating a mixture of **ETTA** and terephthalaldehyde (1:2) in dioxane−acetic acid (aq., 6 M) (1/0.1, v/v) binary solvent in a sealed glass ampule at 120 °C for 96 h gave a yellow powder in 90.2% isolation yield (see details in Supporting Information). The resulting powder was insoluble in common organic solvents. It exhibited high stability in aqueous and common organic solvents and remained intact when it was stored in air for 2 weeks (Figures S1 and S2 in Supporting Information). Thermogravimetric analysis (TGA) revealed that the as-prepared COF was thermostable. More than 95% weight was maintained when the temperature increased from 35 to 475 °C (Figure S3 in Supporting Information).

The as-prepared COF was first characterized by Fourier transform infrared spectroscopy (FT-IR), which showed the stretching vibration band of C═N at 1618 cm^{-1}, confirming the formation of C═N linkage (Figure S4 in Supporting Information). Elemental analysis of the COF revealed that contents of hydrogen, carbon, and nitrogen of the COF were 5.00%, 82.89%, and 9.08%, respectively, which were close to their corresponding theoretical values (4.79% for H, 85.69% for C, and 9.52% for N) calculated for an infinite 2D sheet. Solid-state ^{13}C CP-MAS NMR spectroscopy (Figure S5 in Supporting Information) revealed a characteristic resonance signal at 156 ppm, further confirming the presence of C═N bonds formed by the condensation of the starting materials. The morphology of the COF was investigated by scanning electron microscopy (SEM), and sheet-like morphology was observed, again indicating the formation of 2D sheet structure (Figure S6 in Supporting Information).

In order to determine the exact periodical structure of the as-prepared COF, simulation of PXRD was carried out by using Reflex in Accelrys Material Studio 7.0 software package to predict which kind of unit cell the COF will generate (see details in Supporting Information). In the simulation, there are two possible crystal systems for COFs fabricated from **ETTA** and terephthalaldehyde: orthorhombic and hexagonal (Figure 1). For the orthorhombic system, both eclipsed structure (**AA-O**) and staggered structure (**AB-O**), with unit cell parameters of a = 29.2 Å, b = 25.4 Å, c = 4.8 Å (**AA-O**) or 9.6 Å (**AB-O**), and $\alpha = \beta = \gamma = 90°$, were constructed after the geometry optimization by semiempirical calculations at PM3 level. For hexagonal system, both eclipsed structure (**AA-H**) and staggered structure (**AB-H**), with unit cell parameters of $a = b$ = 37.9 Å, c = 4.8 Å (**AA-H**) or 9.6 Å (**AB-H**), $\alpha = \beta = 90°$, and $\gamma = 120°$, were constructed to generate simulated PXRD pattern, which gave (100) peak at 2θ = 2.76°. PXRD experiment was then performed for the as-prepared COF, and the experimentally observed PXRD pattern was compared with the calculated ones (Figure 1a−f). Notably, the experimental PXRD pattern exclusively reproduced the simulated PXRD pattern of the **AA-H** structure (Figure 1a−c), strongly suggesting that the as-prepared COF holds a dual-pore structure. As expected, in the experimental PXRD profile, the (100) peak at 2.78° exhibited the strongest diffraction intensity, indicating that the highly periodic structure existed in the COF. In addition to the (100) peaks, diffraction peaks at 5.43°, 8.14°, and 10.85° were also observed, which were assignable to 200, 300, and 400 facets, respectively. The (100), (200), and (300) peaks were also corroborated by small-angle X-ray scattering (SAXS) experiment (Figure S7 in Supporting Information). Moreover, the stacking of the 2D sheets (001

dx.doi.org/10.1021/ja5092936 | J. Am. Chem. Soc. 2014, 136, 15885−15888

facet) was also observed with interlayer distance being about 4.4 Å (2θ around 18.7°) (Figure 1). The broad peak of (001) suggests the existence of stacking faults between the 2D sheets.[26] The experimental PXRD pattern was refined by Pawley method to yield cell parameters $a = b = 37.6753$ Å and $c = 4.7576$ Å with $R_p = 3.35\%$ and $R_{wp} = 4.33\%$, which were consistent with the cell parameters generated by the simulation.

Another key evidence for the formation of dual-pore COF was provided by nitrogen adsorption–desorption experiment. As shown in Figure 2a, the N_2 isotherm of the as-prepared

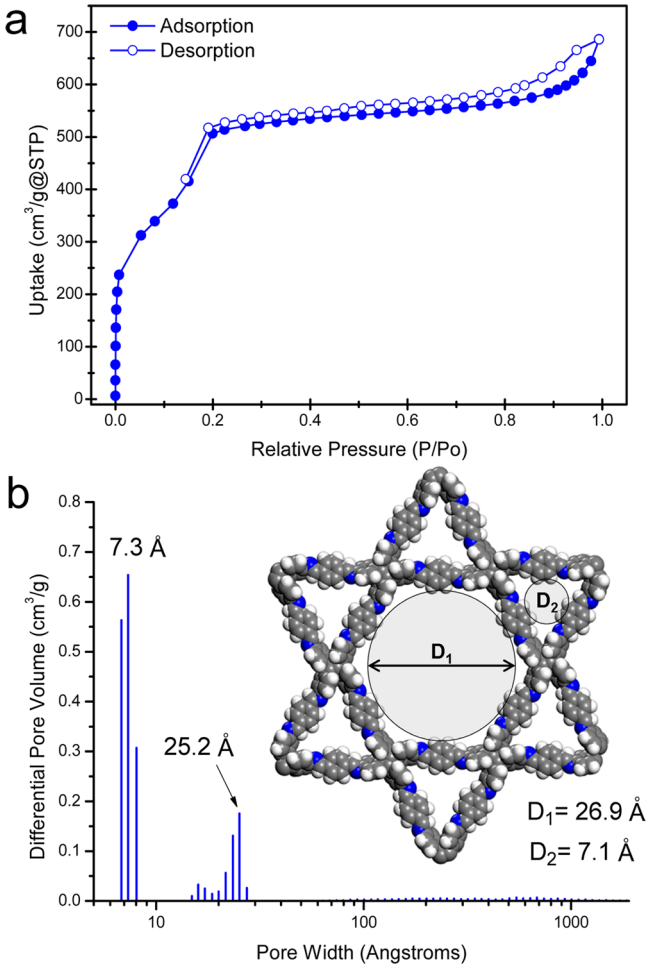

Figure 2. (a) N_2 adsorption and desorption isotherm curves and (b) pore size distribution profile of the dual-pore COF.

COF showed a sharp uptake below $P/P_0 = 0.01$ with a step between $P/P_0 = 0.15–0.20$. The whole curve exhibited a combination of type I and IV nitrogen sorption isotherms,[27] indicating that this material possessed both microporous and mesoporous characters. The maximum N_2 uptake of the COF reached 686.1 cm^3/g (Figure 2a). Brunauer–Emmett–Teller (BET) model was applied to the isotherm for P/P_0 between 0.05 and 0.3, which generated a BET surface area of 1771.38 m^2/g (Figure S8 in Supporting Information). The total pore volume of the COF was calculated to be 3.189 cm^3/g ($P/P^0 = 0.99$). Its porosity was reflected by pore size distribution obtained from nitrogen adsorption–desorption analysis. Fitting the data with nonlocal density functional theory (NLDFT) calculation revealed two narrow pore size distributions at 7.3 and 25.2 Å, respectively (Figure 2b). They are very close to the theoretical values of 7.1 and 26.9 Å estimated by PM3 calculations. This result corroborated again the formation of dual-pore COF. The larger diameter was assigned to the hexagonal pores, and the smaller one could be assigned to the triangle pores. On the basis of the comparison of theoretical and experimental PXRD patterns and the result from the nitrogen adsorption–desorption experiment, the obtention of dual-pore COF, which holds the structure as illustrated by **AA-H** in Figure 1g, could be confirmed. Hydrogen uptake capacity of this dual-pore COF was investigated. H_2 adsorption–desorption isotherms collected at 77 K revealed a H_2 uptake of 1.37 wt % at 1 bar, suggesting its potential application for gas storage (Figure S9 in Supporting Information).

The reason why only the eclipsed dual-pore structure (**AA-H**) was generated was provided by molecular mechanics calculations, which were performed by using COMPASS II as the force field in Forcite of Material Studio 7.0. The results for the relative values of total energy for the four possible structures, which are the **AA-H**, **AB-H**, **AA-O**, and **AB-O**, are provided in Table 1. As can be seen from the table, the

Table 1. Relative Total Energies of the Four Possible COF Structures Generated by Molecular Mechanic Calculations

structure	AA-H	AB-H	AA-O	AB-O
relative total energy (kcal/mol)	0	25.2	199.1	90.1

structures of the hexagonal system (**AA-H** and **AB-H**) gave much lower energy than that of orthorhombic system, and **AA-H** structure is thermodynamically the most stable one. In this context, only the thermodynamically most stable product, that is, dual-pore COF, was produced. It should be pointed out that such dual-pore structure was not observed for the COFs fabricated from monomers having similar symmetries as the ones used in this work.[28] Instead, in those systems, products with single-pore structures were generated exclusively. It could be attributed to the different chemical structures of the monomers, which result in different relative total energies of the products, albeit their symmetries are similar. To validate it, molecular mechanics calculations were also performed for one representative of those COFs reported by Jiang et al.[28] The result indeed revealed that the COF with single-pore structure was thermodynamically the most stable one in Jiang's system (Figures S10 and S11 and Table S3 in Supporting Information). This result suggests that the change in the chemical structure of monomer may induce dramatic change in the topological structure of COF.

In conclusion, for the first time, a 2D dual-pore COF, which possesses both micropores and mesopores, has been constructed in a one-step synthesis. It bears hexagonal pores of 26.9 Å and triangle pores of 7.1 Å, and the pores distribute alternately and periodically in the 2D sheets. The unique dual-pore feature of this new type of COF should bring some novel functions, for example, multiselectivity, and should be useful in adsorption and separation science. Furthermore, employing the same principle, the fabrication of other dual-pore COFs with controllable pore sizes could be expected by the delicate design of monomers. These potentials are under investigation in our laboratory.

dx.doi.org/10.1021/ja5092936 | J. Am. Chem. Soc. 2014, 136, 15885–15888

■ ASSOCIATED CONTENT

Supporting Information

Procedure for the preparation of the dual-pore COF, FT-IR spectra, solid-state ^{13}C CP-MAS NMR spectrum, SEM image, TGA trace, SAXS profile, structural simulation and PXRD analysis, and relative total energies of the possible COF structures for the reference monomers. This material is available free of charge via the Internet at http://pubs.acs.org.

■ AUTHOR INFORMATION

Corresponding Author

*xzhao@sioc.ac.cn

Notes

The authors declare no competing financial interest.

■ ACKNOWLEDGMENTS

We thank the National Natural Science Foundation of China (Nos. 21172249 and 91127007) for financial support.

■ REFERENCES

(1) Côté, A. P.; Benin, A. I.; Ockwig, N. W.; O'Keeffe, M.; Matzger, A. J.; Yaghi, O. M. *Science* **2005**, *310*, 1166.
(2) Ding, S.-Y.; Wang, W. *Chem. Soc. Rev.* **2013**, *42*, 548.
(3) Biswal, B. P.; Chandra, S.; Kandambeth, S.; Lukose, B.; Heine, T.; Banerjee, R. *J. Am. Chem. Soc.* **2013**, *135*, 5328.
(4) Kandambeth, S.; Mallick, A.; Lukose, B.; Mane, M. V.; Heine, T.; Banerjee, R. *J. Am. Chem. Soc.* **2012**, *134*, 19524.
(5) Neti, V. S. P. K.; Wu, X.; Deng, S.; Echegoyen, L. *Polym. Chem.* **2013**, *4*, 4566.
(6) Nagai, A.; Guo, Z.; Feng, X.; Jin, S.; Chen, X.; Ding, X.; Jiang, D. *Nat. Commun.* **2011**, *2*, 536.
(7) Ding, S.-Y.; Cao, J.; Wang, Q.; Zhang, Y.; Song, W.-G.; Su, C.-Y.; Wang, W. *J. Am. Chem. Soc.* **2011**, *133*, 19816.
(8) Fang, Q.; Gu, S.; Zheng, J.; Zhuang, Z.; Qiu, S.; Yan, Y. *Angew. Chem., Int. Ed.* **2014**, *53*, 2878.
(9) Wan, S.; Gándara, F.; Asano, A.; Furukawa, H.; Saeki, A.; Dey, S. K.; Liao, L.; Ambrogio, M. W.; Botros, Y. Y.; Duan, X.; Seki, S.; Stoddart, J. F.; Yaghi, O. M. *Chem. Mater.* **2011**, *23*, 4094.
(10) Ding, X.; Guo, J.; Feng, X.; Honsho, Y.; Guo, J.; Seki, S.; Maitarad, P.; Saeki, A.; Nagase, S.; Jiang, D. *Angew. Chem., Int. Ed.* **2011**, *50*, 1289.
(11) Chen, L.; Furukawa, K.; Gao, J.; Nagai, A.; Nakamura, T.; Dong, Y.; Jiang, D. *J. Am. Chem. Soc.* **2014**, *136*, 9806.
(12) Zhou, T.-Y.; Lin, F.; Li, Z.-T.; Zhao, X. *Macromolecules* **2013**, *46*, 7745.
(13) El-Kaderi, H. M.; Hunt, J. R.; Mendoza-Cortés, J. L.; Côté, A. P.; Taylor, R. E.; O'Keeffe, M.; Yaghi, O. M. *Science* **2007**, *316*, 268.
(14) Bertrand, G. H. V.; Michaelis, V. K.; Ong, T. C.; Griffin, R. G.; Dincă, M. *Proc. Natl. Acad. Sci. U.S.A.* **2013**, *110*, 4923.
(15) Uribe-Romo, F. J.; Hunt, J. R.; Furukawa, H.; Klöck, C.; O'Keeffe, M.; Yaghi, O. M. *J. Am. Chem. Soc.* **2009**, *131*, 4570.
(16) Zhang, Y.-B.; Su, J.; Furukawa, H.; Yun, Y.; Gándara, F.; Duong, A.; Zou, X.; Yaghi, O. M. *J. Am. Chem. Soc.* **2013**, *135*, 16336.
(17) Das, G.; Shinde, D. B.; Kandambeth, S.; Biswal, B. P.; Banerjee, R. *Chem. Commun.* **2014**, *50*, 12615.
(18) Liu, X.-H.; Guan, G.-Z.; Ding, S.-Y.; Wang, W.; Yan, H.-J.; Wang, D.; Wan, L.-J. *J. Am. Chem. Soc.* **2013**, *135*, 10470.
(19) Uribe-Romo, F. J.; Doonan, C. J.; Furukawa, H.; Oisaki, K.; Yaghi, O. M. *J. Am. Chem. Soc.* **2011**, *133*, 11478.
(20) Rowan, S. J.; Cantrill, S. J.; Cousins, G. R. L.; Sanders, J. K. M.; Stoddart, J. F. *Angew. Chem., Int. Ed.* **2002**, *41*, 898.
(21) Tilford, R. W.; Mugavero, S. J.; Pellechia, P. J.; Lavigne, J. J. *Adv. Mater.* **2008**, *20*, 2741.
(22) Lanni, L. M.; Tilford, R. W.; Bharathy, M.; Lavigen, J. J. *J. Am. Chem. Soc.* **2011**, *133*, 13975.
(23) Spitler, E. L.; Koo, B. T.; Novotney, J. L.; Colson, J. W.; Uribe-Romo, F. J.; Gutierrez, G. D.; Clancy, P.; Dichtel, W. R. *J. Am. Chem. Soc.* **2011**, *133*, 19416.
(24) Spitler, E. L.; Dichtel, W. R. *Nat. Chem.* **2010**, *2*, 672.
(25) Two-dimensional COFs bearing two kinds of pores have been reported recently. However, in those COFs, the smaller pore was introduced by a cyclic monomer (9,10-hydroxyphenanthrene cyclotrimer), not formed by condensation reaction of the monomers. Furthermore, the smaller pore is too small to accommodate guest molecules. See Feng, X.; Dong, Y.; Jiang, D. *CrystEngComm* **2013**, *15*, 1508.
(26) Côté, A. P.; EI-Kaderi, H. M.; Furukawa, H.; Hunt, J. R.; Yaghi, O. M. *J. Am. Chem. Soc.* **2007**, *129*, 12914.
(27) Sing, K. S. W.; Everett, D. H.; Haul, R. A. W.; Moscou, L.; Pierotti, R. A.; Rouquérol, J.; Siemieniewska, T. *Pure Appl. Chem.* **1985**, *57*, 603.
(28) Chen, X.; Huang, N.; Gao, J.; Xu, H.; Xu, F.; Jiang, D. *Chem. Commun.* **2014**, *50*, 6161.